A Partial Shading Detection Algorithm for Photovoltaic Generation Systems

Alireza Zabihi[a,b], Iman Sadeghkhani[a,b,*], Bahador Fani[a,b]

[a]*Smart Microgrid Research Center, Najafabad Branch, Islamic Azad University, Najafabad 85141-43131, Iran*
[b]*Department of Electrical Engineering, Najafabad Branch, Islamic Azad University, Najafabad 85141-43131, Iran*

Abstract

Photovoltaic (PV) systems have been gaining great attention during the last decade. One of the main faults in PV arrays is partial shading, affecting its electrical parameters. Failure to detect this fault may result in optimal generated power reduction and hot spotting leading to damage to cell encapsulant and second breakdown. This paper develops a partial shading detection algorithm that only requires the available measurements of array voltage and current. By quantifying the wave-shape of the super-imposed component of PV array power by the skewness function, it can discriminate a partial shading condition from the short-circuit and high-resistance faults. The developed scheme is implemented in a central intelligent electronic device and does not require a communication link and training data set. The merits of the proposed partial shading detection algorithm are demonstrated through several fault scenarios using a 5×5 grid-connected PV generation system.

Introduction

According to the international energy agency (IEA) report, the installed capacity of renewable power increases by 1200 GW from 2019 to 2024 which is equal to 50% of renewable power installed capacity of the world and 100% of the present installed power capacity of the United States [1]. Sixty percent of this expected renewable power growth is dedicated to photovoltaic (PV) systems while onshore and offshore wind powers contribute only 25% and 4% of the increase, respectively. This significant attention is due to advances in PV modules, government incentives, and accessibility [2, 3]. PV systems can operate in both grid-connected and islanded (standalone) operating conditions, increasing the power quality and reliability of electrical distribution networks. However, some technical challenge s should be addressed to facilitate the integration of photovoltaic systems into distribution networks.

The outdoor installation makes PV systems vulnerable to various threats [4]. One of the main problems is the occurrence of the partial shading condition (PSC) where a PV array is partially shaded by passing clouds and nearby buildings [5, 6]. If this fault remains undetected, the temperature of the shaded section significantly increases, degrading the PV performance. This phenomenon that is known as hot spotting results in damage to cell encapsulant and second breakdown [7]. On the other hand, PSC causes the presence of multi peaks in *P-V* characteristic curve of PV array, resulting in a deviation from the optimal power generation.

Up to now, various partial shading condition detection methods have been proposed that can be broadly classified into two groups: (i) electrical

*sadeghkhani@pel.iaun.ac.ir

parameter processing based techniques and (ii) machine learning-based techniques. In the first group, mainly a PSC detection index is defined and by comparing it with a threshold. The conventional partial shading condition detection criterion is an abrupt change of PV output power. However, the low value of power change in large PV systems and malfunction in the case of a short-circuit fault are the disadvantages of this method. The partial shading condition detection criteria proposed in [8] consist of the derivative of array power with respect to array voltage and change of array and module voltages. By comparing the measured and simulated losses of the PV system, [9] presents a partial shading condition detection scheme. A modified beta method is proposed in [10] to detect PSC. By monitoring the slope of *I-V* characteristic curve, [11, 12] detect the partial shading condition. The partial shading condition detection technique proposed in [13] compares the output power of PV modules using communication between their converters. The basis of the second group is to apply machine learning techniques. The artificial neural network (ANN) is used in [14] to detect partial shading conditions. Using the *I-V* curve and environmental parameters, a kernel-based extreme learning machine is trained in [15] to detect PSC. Based on parameters calculated from the *I-V* characteristic curve, [16] presents a PSC detection method using a fuzzy classifier. In [17], a voltage based shading pattern and a multiple-output support vector regression are used to estimate the shading rate and shading strength, respectively. A PSC detection technique based on the decision tree model is developed in [18]. The need for training data set is the main disadvantage of the second PSC detection group.

This paper presents an online electrical parameter processing based technique for PSC detection. By measuring the available measurements of PV voltage and current, the output power of the PV array is calculated and adopted as the electrical parameter o be processed. First, the super-imposed component of PV power is calculated by a central intelligent electronic device (IED) to detect a fault condition. Then, it is used as the input of skewness function to quantify its wave-shape, classifying the fault condition. The developed method does not require training data set and communication links and does not mal-operate in the case of short-circuit fault.

The rest of the paper is organized as follows. The partial shading condition is described in the Partial Shading Condition Section. Developed Methodology Section is dedicated to the proposed PSC detection strategy. The performance of the developed scheme is assessed in the Performance Evaluation Section. Finally, Conclusion Section concludes the paper.

Partial Shading Condition

A PV array consists of several strings where each string comprises a group of PV modules. Each PV module is composed of several PV cells. Due to the small area of a PV array, it receives uniform solar irradiation during the normal operating condition. In this condition, the single-diode equivalent circuit is generally used to model each PV module as [19]

$$I = I_{ph} - I_0 \left[\exp\left(\frac{q(V + R_S I)}{nk_B T} \right) - 1 \right] - \frac{V + R_S I}{R_{sh}},$$

(1)

where I and V are the output current and voltage, I_{ph} and I_0 are the light-generated and diode reverse saturation currents, q and T are the electronic charge and cell's temperature, n and k_B are the diode's ideality factor and Boltzmann constant, and R_{sh} and R_S are the shunt and series resistances, respectively. Each PV module is characterized by two curves of current-voltage (*I-V*) and power-voltage (*P-V*). Based on (1), the generated current (power) of a PV module depends on solar irradiation. Fig. 1 shows the characteristic curves of a PV string with five series 305.2 W SunPower modules under various irradiations. The open-circuit voltage V_{OC}, short-circuit current I_{SC}, voltage at maximum power point (MPP) V_{MPP}, and current at maximum power point I_{MPP} of each module are 64.2 V, 5.96 A, 54.7 V, and 5.58 A, respectively. As shown in Fig. 1, the maximum generated power of the study PV string (MPP) changes by variation of solar irradiance.

However, due to outdoor installation, PV arrays are always vulnerable to partial shading conditions, resulting in non-uniform irradiation conditions. A partial shading condition is characterized by two factors [17]: shading rate χ and shading strength ρ. The shading rate determines the percentage of shaded modules in a string as
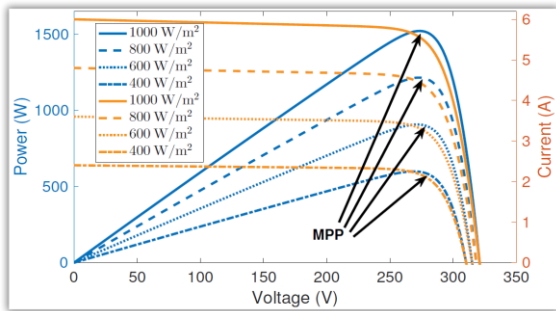
$$\chi = \frac{N_{shaded}}{N_S} \times 100,$$

(2)

Figure 1. PV characteristic curves under uniform solar irradiation.

where N_{shaded} is the number of shaded modules in a string and N_S is the number of all modules of a string. The shading strength determines the percentage of solar irradiance reduction on the shaded modules with respect to the standard test condition (STC, 1000 W/m² irradiation and 25°C temperature) as

$$\rho = \frac{G_{shading}}{G_{STC}} \times 100, \qquad (3)$$

where $G_{shading}$ is the solar irradiance at shaded modules and G_{STC} is the solar irradiance under STC.

Fig. 2 shows the characteristic curves of study PV string under various shading rates while in Fig. 3, the characteristic curves are shown in the case of two shaded modules with various shading strengths. When a partial shading occurs, there is more than one MPP in the characteristic curves (in this case 2 MPPs) where one MPP is the global MPP with the highest power while others are local MPPs with lower power. The conventional maximum power point tracking (MPPT) algorithms may not be able to find the global MPP, resulting in a reduction of injected power of PV arrays to the distribution network. Fig. 4 shows the characteristic curves of the study PV string when four modules are shaded by ρ of 5%, 15%, 25%, and 35%. In this case, there are 5 MPPs, making the global MPP determination difficult.
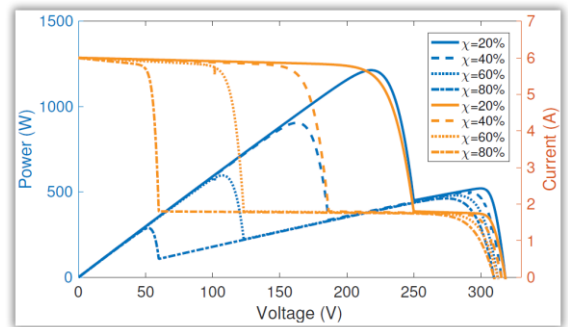

Figure 2. PV characteristic curves under various shading rates.
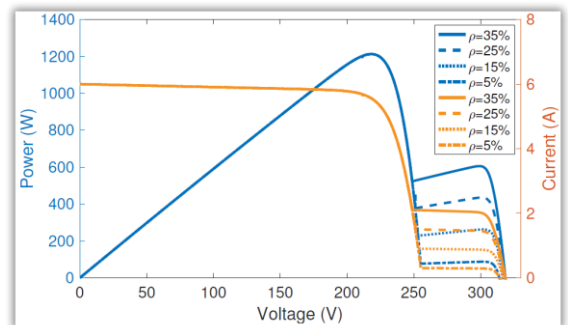

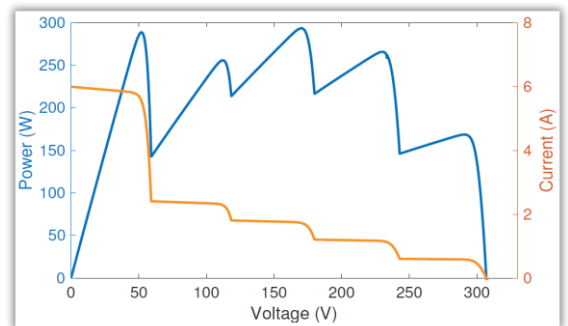Figure 3. PV characteristic curves under various shading strengths.

Figure 4. PV characteristic curves in the case of non-uniform shading condition.

On the other hand, when a module is shaded, its I-V curve shifts down, as shown in Fig. 1. In this condition, the module voltage becomes negative and the modules consume power instead of power generation, as shown in Fig. 5. The power dissipation results in temperature increment. If the partial shading condition is present for a long time, the hot spotting phenomenon occurs, resulting in damage to the shaded PV modules. Although the installation of bypass diodes in parallel with PV modules can mitigate hot spotting, additional cost

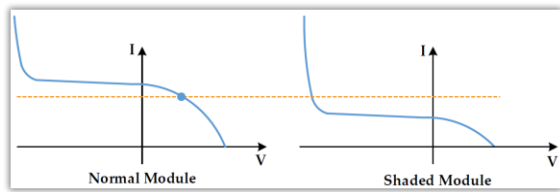and power loss of bypass diodes limit their application.

Figure 5. *I-V* characteristic curves of series normal and shaded modules.

Developed Methodology

According to the previous section, a partial shading condition may result in generated power reduction and damage to PV modules. To address these problems, the protection system of PV arrays should be equipped with a partial shading condition detection unit. This paper presents a partial shading detection algorithm using the statistical measure of skewness. By monitoring a moving data window consisting of the superimposed component of PV power, its wave-shape is quantified as the partial shading detection index. The remainder of this section is dedicated to the mathematical description of the proposed two-stage strategy.

Stage 1 - Fault Detection: The proposed scheme only requires available measurements of PV array voltage and current; thus, it does not impose the additional cost. The first step is to mitigate the noise by passing the recorded voltage and current signals through the low-pass filters (LPFs). The processing of the filtered signals is done by a central IED. It samples the PV voltage and current signals with a sampling frequency of f_s. The sampled signals are normalized as

$$v_{PV}^{pu}[k] = \frac{v_{PV}}{V_{OC}}, \tag{4}$$

$$i_{PV}^{pu}[k] = \frac{i_{PV}}{I_{SC}}, \tag{5}$$

where v_{PV} and i_{PV} are the array voltage and current and v_{PV}^{pu} and i_{PV}^{pu} are their normalized value, respectively. k is the sampling step. By using (4) and (5), the normalized PV array power p_{PV}^{pu} is calculated as

$$p_{PV}^{pu}[k] = v_{PV}^{pu}[k] \times i_{PV}^{pu}[k]. \tag{6}$$

To simplify the detection of an abnormal condition, the super-imposed component of array power is calculated. Based on superposition theorem, the PV power during a fault condition comprises of normal running and super-imposed components as [20]

$$p_{PV,F}^{pu}[k] = p_{PV,N}^{pu}[k] \times p_{PV,SI}^{pu}[k], \tag{7}$$

where $p_{PV,F}^{pu}$, $p_{PV,N}^{pu}$, and $p_{PV,SI}^{pu}$ are the fault, normal running, and super-imposed components of PV array power, respectively. Using the Delta filter [20], the super-imposed power can be calculated as

$$p_{PV,SI}^{pu}[k] = p_{PV}^{pu}[k] \times p_{PV}^{pu}[k - k_d], \tag{8}$$

where k_d is the number of time delay samples. The promising feature of the super-imposed component is that it is about zero during normal operation while it changes when a disturbance occurs. Consequently, a fault condition is verified if $\left| p_{PV,SI}^{pu} \right| > \xi_1$, where ξ_1 is the fault detection threshold.

Stage 2 - Fault Classification: The super-imposed power is not a reliable detection index because it changes for every fault such as partial shading and short-circuit conditions. To address this problem, this paper proposes to use the skewness. As a statistical measure, it quantifies the spread of data around the mean. If the skewness is positive (negative), the signal is more shifted to the right (left) while if the data has the normal distribution, the skewness is zero.

In the proposed scheme, the super-imposed power is monitored in a moving data window with a length of N. The jth window is formed as

$$\mathbf{P}_j = \left[\left| p_{PV,SI}^{pu}[j-1] \right| \quad \cdots \quad \left| p_{PV,SI}^{pu}[j-N] \right| \right]. \tag{9}$$

To quantify the asymmetry of the $\mathbf{P}_j$ around the mean μ, the skewness S of set $\mathbf{P}_j$ is calculated as [21]

$$S\left(\mathbf{P}_j\right)=\frac{E\left(\mathbf{P}_j-\mu_j\right)^3}{\sigma_j^3}, \tag{10}$$

where E is the expected value of $\mathbf{P}-\mu$ and σ is the standard deviation. During normal operation, the super-imposed power is not exactly zero due to small disturbance of non-ideal filtering. Thus, the skewness of super-imposed power data is non-zero during normal operation. When a disturbance occurs in the PV array, it changes to another non-zero value. It makes threshold determination difficult. To address this problem, the super-imposed component of skewness S_{SI} is calculated as

$$S_{SI,j}=S\left(\mathbf{P}_j\right)-S\left(\mathbf{P}_{j-1}\right). \tag{11}$$

During normal operation, data of two subsequent moving window data are very similar, resulting in similar skewness values and nearly zero S_{SI}. However, when a disturbance occurs, S_{SI} changes and has a non-zero value.

When a short-circuit fault occurs, the super-imposed power changes instantaneously while it varies slower during partial shading conditions. The reason is that the dynamic model of the PV cell comprises a shunt resistance in parallel with a small leakage capacitor. Thus, the PV cell natural transient response has a sigmoid-like "S" shape in the case of partial shading while it has an exponential shape in the case of a short circuit, similar to a first-order circuit [22]. It results in the super-imposed power wave-shape during a partial shading condition is similar to the normal distribution, resulting in the skewness of nearly zero while during a short-circuit condition, the wave-shape of super-imposed power spreads out more to the right, resulting in positive skewness. Consequently, using the fault classification threshold of ξ_2, a partial shading condition can be discriminated from a short-circuit fault. The developed fault classification scheme is expressed as

$$\begin{cases} \text{Partial Shading,} & \left|p_{PV,SI}^{pu}>\xi_1\right| \& S_{SI}<=\xi_2 \\ \text{Short-Circuit,} & \left|p_{PV,SI}^{pu}>\xi_1\right| \& S_{SI}>\xi_2 \\ \text{Normal Condition,} & \text{Otherwise} \end{cases} \tag{12}$$

Fig. 6 shows the flowchart of the developed partial shading detection strategy. First, the array voltage and current signals are filtered by LPFs and then, the central IED samples and normalized them. The absolute value of the super-imposed component of array power is calculated and monitored to detect the abnormal condition. Then, the skewness is calculated for the moving windows of $\mathbf{P}_j$. Based on (12), the PV operating condition is classified.

Performance Evaluation
To assess the performance of the proposed partial shading detection algorithm, a 5×5, 7.6 kW PV array is simulated in MATLAB/Simulink environment. The 305.2 W SunPower modules are made of mono-crystalline cells. Fig. 7 shows the layout of the study grid-connected PV array. It consists of DC-DC and DC-AC converters. The control system of the 500 V DC-DC converter aims to track the MPP by the peuterb and observation (P&O) MPPT algorithm [23]. The DC-AC converter is the interface between the DC side of the study array and distribution network. It is a centralized three-phase three-level voltage-sourced converter (VSC) with two control loops to regulate the DC link voltage and real and reactive components of the distribution network current. The developed algorithm is implemented in central IED with the following parameters: the sampling frequency f_s of 1 kHz, moving window length N of 200, time delay sample number k_d of 50, fault detection threshold ξ_1 of 0.004 pu, and fault classification threshold ξ_2 of 1.4.
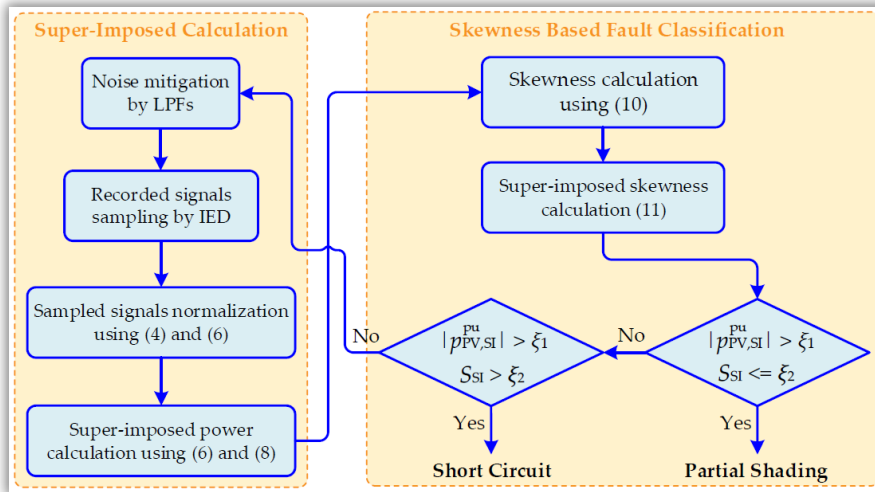
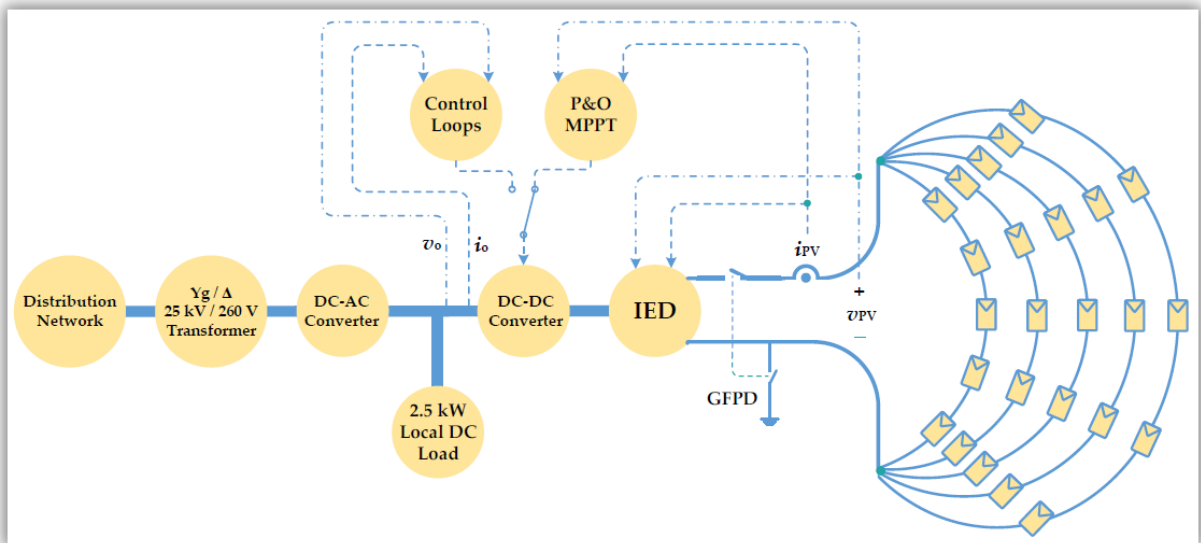Figure 6. Flowchart of the developed partial shading condition detection algorithm.

Figure 7. Layout of the study grid-connected PV array.

Case 1 - Partial Shading: This section is dedicated to evaluating the performance of the developed algorithm in the case of partial shading conditions. First, a severe partial shading condition is simulated. To this end, 3 out of 5 strings are adopted and in each string, 4 out of 5 modules are shaded, i.e, about 50% of the study PV array is under partial shading condition. The simulated shading starts at $t = 0.7$ s and during 0.3 s, the solar irradiance for shaded modules is reduced from 1000 W/m² to 100 W/m². Thus, the shading rate is $\chi = 80\%$ and the final

shading strength is $\rho = 10\%$. The simulation results are shown in Fig. 8. $\left| p_{\text{PV,SI}}^{\text{pu}} \right|$ increase to 0.09 pu and exceeds fault detection threshold ξ_1. However, due to the low speed of super-imposed power change, the super-imposed power wave-shape is similar to the normal distribution, resulting in the low super-imposed skewness of 1.07 that is lower than the fault classification threshold ξ_2. Consequently, this condition is properly classified as a partial shading.
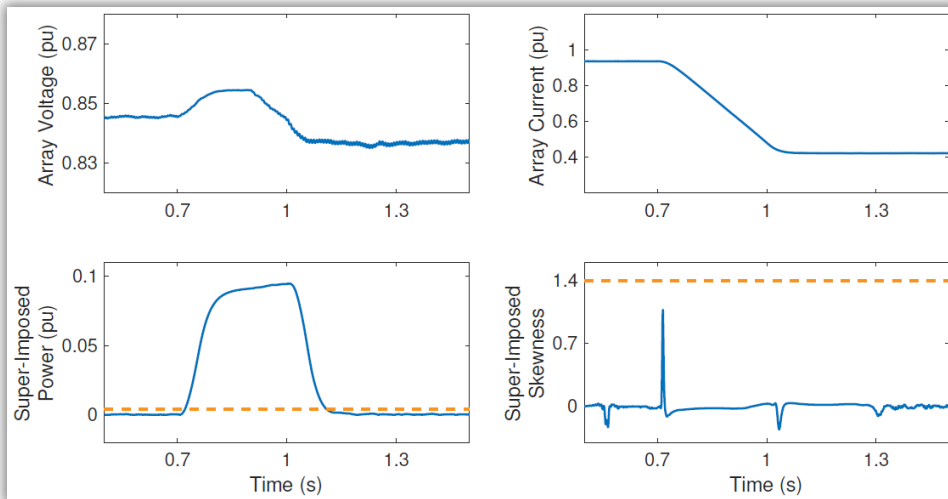
Figure 8. Performance of the developed algorithm in the case of a severe partial shading condition.
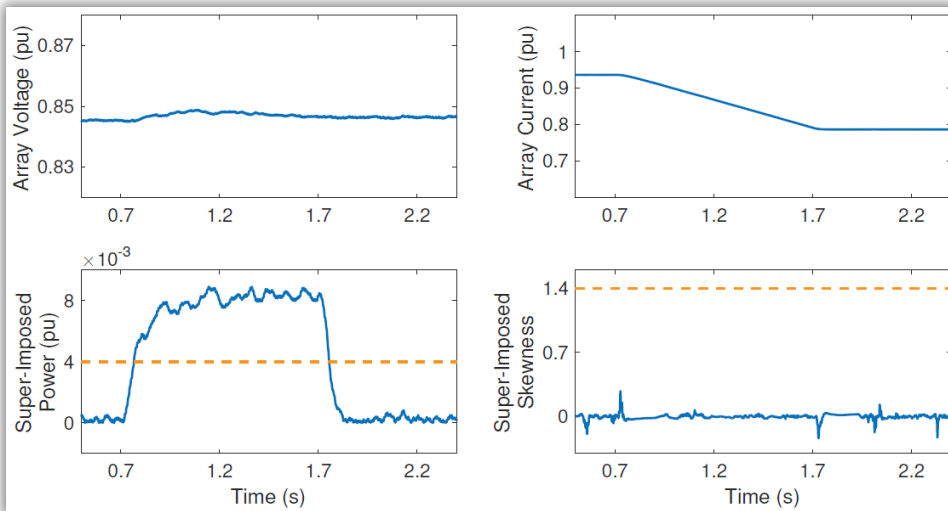

Figure 9. Performance of the developed algorithm in the case of a non-severe partial shading condition.

In the next scenario, a non-severe partial shading condition is considered where 3 modules of only one string are shaded (12% of the study PV array). In this scenario, the solar irradiance for shaded modules is reduced from 1000 W/m² to 200 W/m² during 1 s. Thus, the shading rate and shading strength are 60% and 20%, respectively. Fig. 9

shows the study results. The super-imposed power increases to 0.009 pu and exceeds the fault detection threshold of 0.004 pu. However, S_{SI} is below the fault classification threshold of 1.4. According to (12), the developed algorithm interprets this abnormal condition as a partial shading.
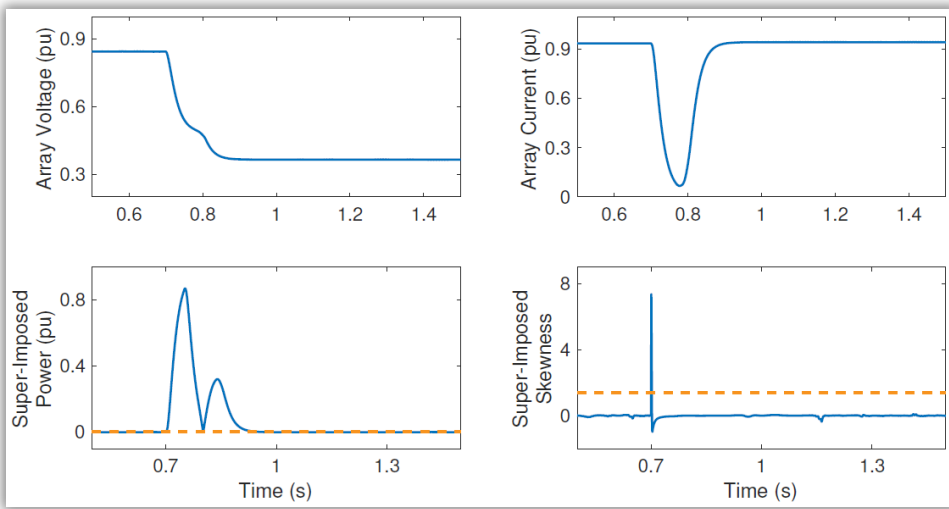
Figure 10. Performance of the developed algorithm in the case of a severe short-circuit condition.
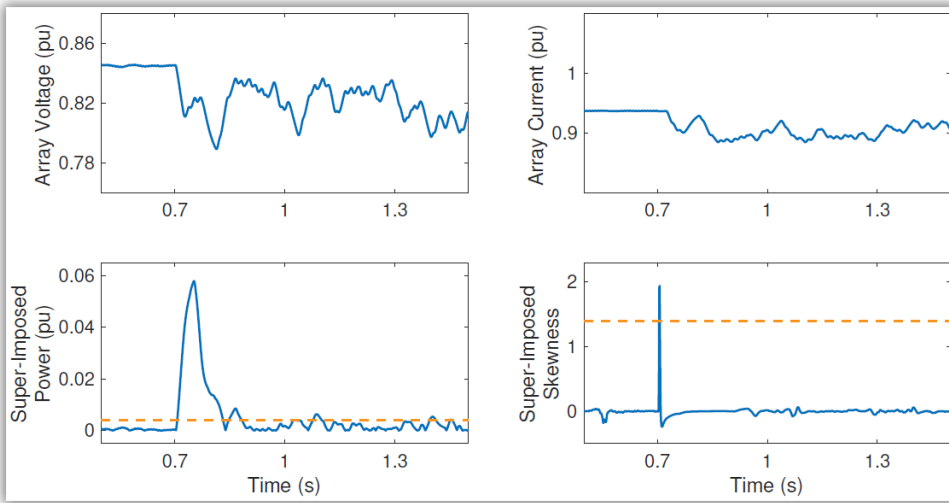

Figure 11. Performance of the developed algorithm in the case of a non-severe fault condition.

Case 2 - Short-Circuit: A reliable partial shading detection algorithm does not mal-operate in the case of a short-circuit fault. This section investigates the performance of the proposed scheme during both low-impedance and high-impedance faults. First, a line-tt-line (LL) fault condition with fault path resistance of 0.1 Ω and a location mismatch of 60% as a severe fault condition is simulated at $t = 0.7$ s. Fig. 10 shows the array voltage and current as well as the absolute value of super-imposed power and super-imposed skewness. The maximum value of $\left| p_{\mathrm{PV,SI}}^{\mathrm{pu}} \right|$ is 0.87 pu which is higher than ξ_1; thus, the disturbance is detected. Also, the super-imposed skewness increases to 7.35 which is significantly

higher than ξ_2. Thus, the developed scheme properly classifies this disturbance as a short-circuit fault.

To evaluate the performance of the proposed method during a high-resistance fault, a 15 Ω line-to-ground fault with a location mismatch of 20% as a non-severe fault condition is simulated in the study PV array. The simulation results are shown in Fig. 11. The absolute value of super-imposed power increases to 0.058 pu and the disturbance is detected. S_{SI} is 1.94 for this case, verifying proper classification of the proposed scheme as a short-circuit fault.
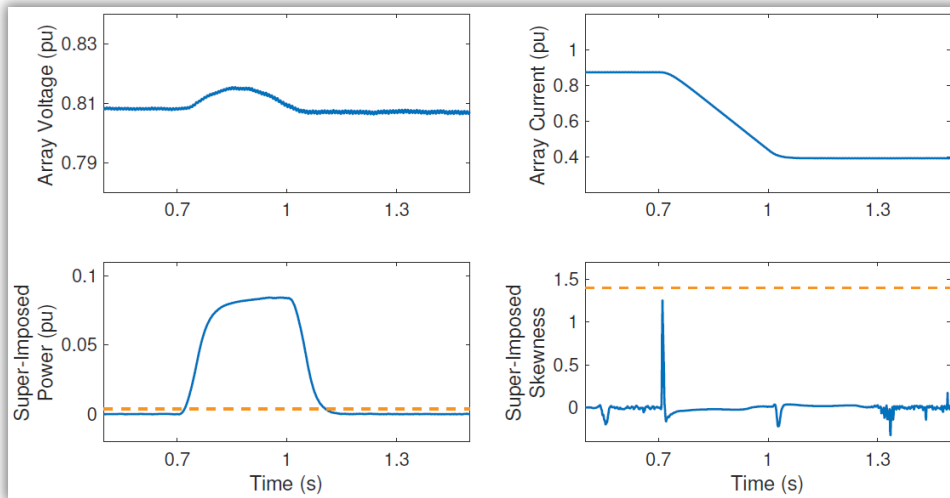
Figure 12. Performance of the developed algorithm in the case of a severe partial shading condition considering parameter uncertainty.

Case 3 - Parameter Uncertainty: Since the PV arrays work for a long time, they are vulnerable to aging, resulting in gradual performance loss [24, 25]. Ref. [26] indicates that for a crystalline silicon system after 20 years of operation, the open-circuit voltage, short-circuit current, and maximum power reduce by about 3%, 4%, and 11%, respectively. This section is dedicated to evaluating the PV model parameter independency of the proposed partial shading detection scheme. To this end, V_{OC}, I_{SC}, and the maximum power of the PV cells are reduced to 62.2 V, 5.72 A, and 271.5 W, respectively, and the partial shading condition of the first scenario of Case 1 is simulated. According to the simulation results of Fig. 12, this condition is properly detected as a partial shading condition.

Conclusion

The development of an effective protection system paves the way for increased integration of PV generation systems. One of the main protection challenges of PV arrays is the occurrence of partial shading conditions, resulting in optimal power generation reduction and hot spotting. This paper has proposed a wave-shape based partial shading detection algorithm that relies on a central IED, sampling the available measurement of array voltage and current. By quantifying the skewness of super-imposed array power wave-shape, the developed algorithm can detect the partial shading condition and does not mal-operate in the case of short-circuit and high-impedance faults. It does not require a communication link and a training data set. The simulation results of the implementation of the

developed algorithm in a 5×5 grid-connected PV generation system confirm its effectiveness.

References

1. *Renewables 2019*. 2019; Available from: https://www.iea.org/reports/renewables-2019.
2. Chen, L. and X. Wang, *Adaptive Fault Localization in Photovoltaic Systems*. IEEE Transactions on Smart Grid, 2018. **9**(6): p. 6752-6763.
3. Fani, B., H. Bisheh, and I. Sadeghkhani, *Protection coordination scheme for distribution networks with high penetration of photovoltaic generators*. IET Generation, Transmission & Distribution, 2018. **12**(8): p. 1802-1814.
4. Maleki, A., I. Sadeghkhani, and B. Fani, *Statistical sensorless short-circuit fault detection algorithm for photovoltaic arrays*. Journal of Renewable and Sustainable Energy, 2019. **11**(5): p. 053501.
5. Guo, S., et al. *Analysing partial shading of PV modules by circuit modelling*. in *2012 38th IEEE Photovoltaic Specialists Conference*. 2012.
6. Kumar, B.P., et al., *Online Fault Detection and Diagnosis in Photovoltaic Systems Using Wavelet Packets*. IEEE Journal of Photovoltaics, 2018. **8**(1): p. 257-265.
7. Kim, K.A. and P.T. Krein, *Reexamination of Photovoltaic Hot Spotting to Show Inadequacy of the Bypass Diode*. IEEE Journal of Photovoltaics, 2015. **5**(5): p. 1435-1441.

8. Ghasemi, M.A., H.M. Foroushani, and M. Parniani, *Partial Shading Detection and Smooth Maximum Power Point Tracking of PV Arrays Under PSC.* IEEE Transactions on Power Electronics, 2016. **31**(9): p. 6281-6292.

9. Silvestre, S., A. Chouder, and E. Karatepe, *Automatic fault detection in grid connected PV systems.* Solar Energy, 2013. **94**: p. 119-127.

10. Li, X., et al., *Modified Beta Algorithm for GMPPT and Partial Shading Detection in Photovoltaic Systems.* IEEE Transactions on Power Electronics, 2018. **33**(3): p. 2172-2186.

11. Ghanbari, T., *Hot spot detection and prevention using a simple method in photovoltaic panels.* IET Generation, Transmission & Distribution, 2017. **11**(4): p. 883-890.

12. Ghanbari, T., *Permanent partial shading detection for protection of photovoltaic panels against hot spotting.* IET Renewable Power Generation, 2017. **11**(1): p. 123-131.

13. Ghassami, A.A. and S.M. Sadeghzadeh, *A communication-based method for PSC Detection and GMP tracking under PSC.* IEEE Transactions on Industrial Informatics, 2019: p. 1-1.

14. Salem, F. and M.A. Awadallah, *Detection and assessment of partial shading in photovoltaic arrays.* Journal of Electrical Systems and Information Technology, 2016. **3**(1): p. 23-32.

15. Chen, Z., et al., *Intelligent fault diagnosis of photovoltaic arrays based on optimized kernel extreme learning machine and I-V characteristics.* Applied Energy, 2017. **204**: p. 912-931.

16. Spataru, S., et al., *Diagnostic method for photovoltaic systems based on light I–V measurements.* Solar Energy, 2015. **119**: p. 29-44.

17. Ma, J., et al., *Detection and Assessment of Partial Shading Scenarios on Photovoltaic Strings.* IEEE Transactions on Industry Applications, 2018. **54**(6): p. 6279-6289.

18. Zhao, Y., et al. *Decision tree-based fault detection and classification in solar photovoltaic arrays*. in *2012 Twenty-Seventh Annual IEEE Applied Power Electronics Conference and Exposition (APEC)*. 2012.

19. Garoudja, E., et al., *Statistical fault detection in photovoltaic systems.* Solar Energy, 2017. **150**: p. 485-499.

20. Zamani, M.A., A. Yazdani, and T.S. Sidhu, *A Communication-Assisted Protection Strategy for Inverter-Based Medium-Voltage Microgrids.* IEEE Transactions on Smart Grid, 2012. **3**(4): p. 2088-2099.

21. Dokov, S., D.P. Morton, and I. Popova. *Mean-Variance-Skewness-Kurtosis efficiency of portfolios computed via moment-based bounds*. in *2017 International Conference on Information Science and Communications Technologies (ICISCT)*. 2017.

22. Saleh, K.A., et al., *Voltage-Based Protection Scheme for Faults Within Utility-Scale Photovoltaic Arrays.* IEEE Transactions on Smart Grid, 2018. **9**(5): p. 4367-4382.

23. Ahmed, A., et al., *A Fast PV Power Tracking Control Algorithm With Reduced Power Mode.* IEEE Transactions on Energy Conversion, 2013. **28**(3): p. 565-575.

24. Fernandes, C.A.F., et al. *Aging of solar PV plants and mitigation of their consequences*. in *2016 IEEE International Power Electronics and Motion Control Conference (PEMC)*. 2016.

25. Vasić, A., et al. *Aging of the photovoltaic solar cells*. in *2010 27th International Conference on Microelectronics Proceedings*. 2010.

26. Jordan, D.C., et al., *Performance and Aging of a 20-Year-Old Silicon PV System.* IEEE Journal of Photovoltaics, 2015. **5**(3): p. 744-751.